NJC

PAPER

View Article Online
View Journal

Cite this: DOI: 10.1039/c5nj02974k

Homopiperazine sulfamic acid functionalized mesoporous silica nanoparticles (MSNs-HPZ-SO_3H) as an efficient catalyst for one-pot synthesis of 1-amidoalkyl-2-naphthols

Zahra Nasresfahani, Mohammad Zaman Kassaee* and Esmaiel Eidi

Received (in Montpellier, France)
24th October 2015,
Accepted 18th March 2016

DOI: 10.1039/c5nj02974k

www.rsc.org/njc

Mesoporous silica nanoparticles are efficiently functionalized with homopiperazine sulfamic acid. The resulting MSNs-HPZ-SO_3H is employed as a nanocatalyst in one-pot synthesis of 1-amidoalkyl-2-naphthols, through three-component condensation reaction of aromatic aldehydes, amides/urea and β-naphthol, under thermal solvent-free conditions. Characterizations of the catalyst are carried out using XRD, SEM, FT-IR, TGA-DTA and nitrogen adsorption–desorption analysis. This protocol is developed as a safe and convenient alternative method for the synthesis of 1-amidoalkyl-2-naphthols utilizing an ecofriendly catalyst.

Introduction

Multicomponent reactions (MCRs) are very elegant and efficient methods for accessing complex structures in a single synthetic operation from the corresponding building blocks. The MCRs are often carried out in one-pot and designed to go through easy procedures with high atom-economy and great selectivity. This is mostly due to the generation of carbon–carbon and carbon heteroatom bonds.[1] One of these MCRs is the preparation of 1-amidoalkyl-2-naphthols. These compounds and their derivatives which bear 1,3-amino oxygenated functional groups have attracted intense attention. This is due to their ubiquitous role as essential building blocks for a variety of biologically important natural products, synthetic pharmaceuticals, and potent drugs, including a number of nucleoside antibiotics and HIV protease inhibitors.[2] Also, these compounds can be converted into important 'drug-like' materials by amide hydrolysis and formation of aminoalkylnaphthols. The hypertensive and broad cardiac effects of these substrates and their potential biological activities have been evaluated extensively. They include antibiotic,[3] antitumor,[4] analgesic,[5] anticonvulsant,[6] antipsychotic,[7] antimalarial,[8] antihypertensive,[9] and antirheumatic properties.[10] Various improved methods have been developed for the preparation of 1-amidoalkyl-2-naphthols from aldehydes, β-naphthols, and amides or urea, under thermal and sonication conditions. Reported catalysts include *p*-TSA,[11] montmorillonite K10,[12] iodine,[13] $H_4SiW_{12}O_{40}$,[14] dodecylphosphonic acid,[15] cyanuric chloride,[16] $Bi(NO_3)_3{\cdot}5H_2O$,[17] $ZrO(OTf)_2$,[18] P_2O_5,[19] thiamine hydrochloride,[20] $HClO_4$–SiO_2,[21] zwitterionic salts,[22] and Brønsted acidic ionic liquids.[23] However, these procedures have their own drawbacks, such as high reaction temperature, prolonged reaction time, the use of toxic solvents or low yields. Therefore, it is still desirable to seek novel catalysts that are recyclable and capable of performing the reaction under mild conditions. On the other hand, recently mesoporous materials have received much attention, particularly those that are designed based on functionalized mesoporous silicas because of their high surface area, tunable nanoscale pores, ease of the grafting of organic scaffolds to balance between the hydrophilic and hydrophobic character of the porous architecture, exciting host–guest chemistry, and supramolecular interaction to different extents with the reactant molecules.[24,25] Organically functionalized mesoporous silicas have been extensively utilized for the last decade because of their versatile applications in many frontier areas of science like gas storage,[26] proton conduction,[27] uranium sequestration,[28] energy transfer,[29] catalysis,[30–32] Here in, we have developed a synthetic strategy for the design of a homopiperazinesulfamic acid functionalized mesoporous silica (MSNs-HPZ-SO_3H) and its use as an efficient nanocatalyst for the one-pot synthesis of 1-amidoalkyl-2-naphthols *via* three-component reaction of β-naphthol, aldehydes, and amides/urea, under solvent-free conditions.

Results and discussion

In order to reach at MSNs-HPZ-SO_3H, we prepared mesoporous silica nanoparticles (MSNs) *via* sol–gel method.[33] Which it was sequentially treated with 3-chloropropyltriethoxysilane (CPTMS) to give 3-chloropropyl-functionalized (MSNs-Cl). Reaction of the

Department of Chemistry, Tarbiat Modares University, P.O. Box 14155-4838, Tehran, Iran. E-mail: kassaeem@modares.ac.ir, drkassaee@yahoo.com; Fax: +98-21-88006544; Tel: +98-912-1000392

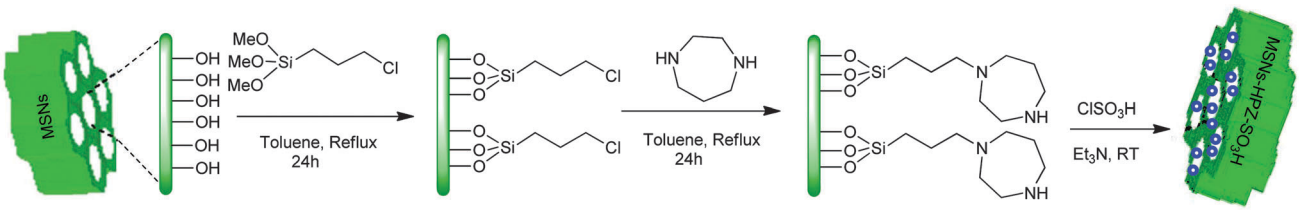

Scheme 1 Preparation of the nanocatalyst (MSNs-HPZ-SO_3H).

latter with homopiperazine gave MSNs-HPZ. Finally, reaction with chlorosulfonic acid ($ClSO_3H$) produced novel nanocatalyst (MSNs-HPZ-SO_3H) (Scheme 1).

Characterization of the catalyst

The as-prepared catalyst is also characterized by Fourier transform infrared spectroscopy (FT-IR), X-ray diffraction (XRD), Scanning electron microscopy (SEM), thermogravimetric/differential thermal analyses (TGA-DTA), nitrogen adsorption–desorption analysis. Reflections in XRD pattern of pure MSNs are assigned to (100), (110), and (200) planes in the highly ordered 2D hexagonal arrangement. The values of *d*-spacing for these XRD peaks appear at 40.01, 26.97 and 22.46 Å, respectively (Fig. 1a). For MSNs-HPZ and MSNs-HPZ-SO_3H only a reflection associated with (100) peak are observed. The intensity of this reflection after functionalizing with HPZ is lower than that of the original MSNs. After loading of sulfonic chloride, the intensity of XRD reflections on MSNs-HPA-SO_3H is weakened further (Fig. 1b).

FT-IR spectra of MSNs, MSNs-Cl, MSNs-HPZ, and MSNs-HPZ-SO_3H are illustrated in Fig. 2. For the parent MSNs, asymmetric and symmetric Si–O–Si characteristic stretching vibrations at 1086 cm^{-1} and 801 cm^{-1} along with Si–OH at 962 cm^{-1} and bending Si–O–Si at 461 cm^{-1} are observed. The broad peak around 3450 cm^{-1} is due to the surface silanols and adsorbed water molecules and the peak at 1635 cm^{-1} is assigned to the H–O–H bending vibration of the free or absorbed water molecules. Stretching vibrations of anchored alkyl groups appear as weak C–H symmetric and asymmetric absorptions at 2930 and 2960 cm^{-1}, respectively. In addition, N–SO_2, O–SO_2 and S=O bonds stretching vibrations should be observed around 1000–1300 cm^{-1}.

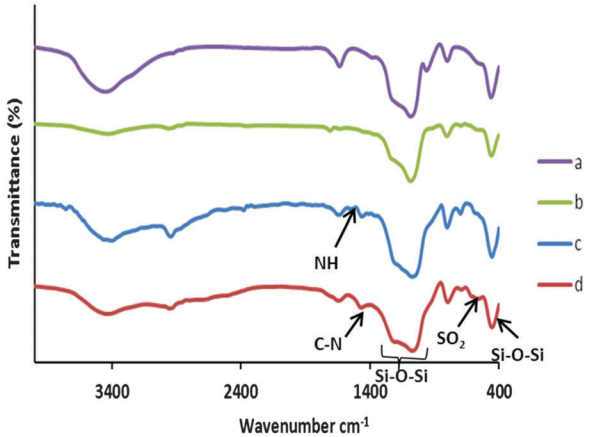

Fig. 2 FT-IR spectra of: (a) MSNs, (b) MSNs-Cl, (c) MSNs-HPZ, (d) MSNs-HPZ-SO_3H.

However, these peaks cannot be resolved due to its overlap with the absorbance of Si–O–Si stretch in the 960–1350 cm^{-1}, broad peak around 2500–3600 cm^{-1} for MSNs-HPZ-SO_3H is due to acidic OH vibration signal of SO_3H. Also, a new band at approximately 580 cm^{-1} is due to the presence of a SO_2 group in MSNs-HPZ-SO_3H (Fig. 2d).

The morphology of the MSNs-HPZ-SO_3H nanocatalyst is investigated by SEM as shown in (Fig. 3a). This micrograph illustrates that the nanoparticles have a semi-spherical morphology. The obtained histogram confirms that the size distribution is narrow with a 23 nm average value and a 17 nm standard deviation (Fig. 3b).

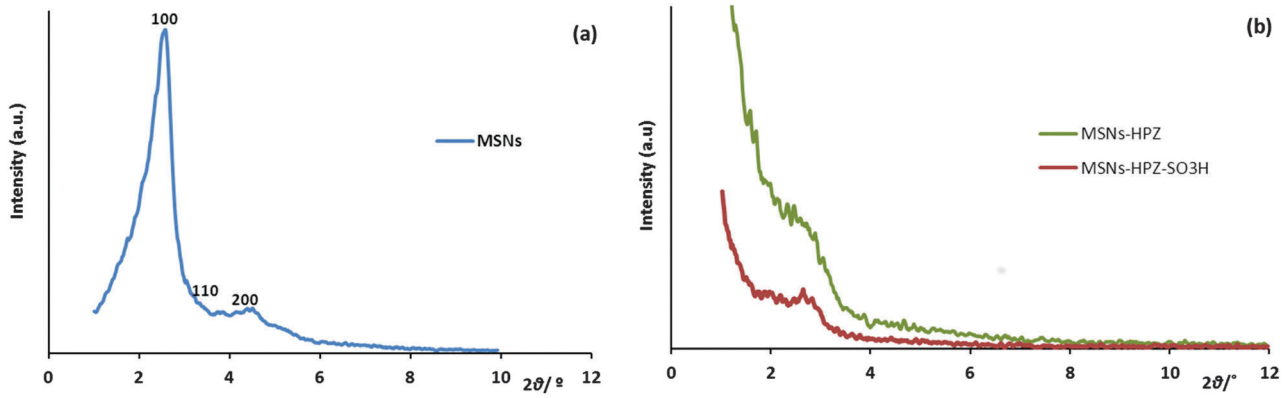

Fig. 1 Small-angle XRD patterns of: (a) MSNs, (b) MSNs-HPZ, and MSNs-HPZ-SO_3H.

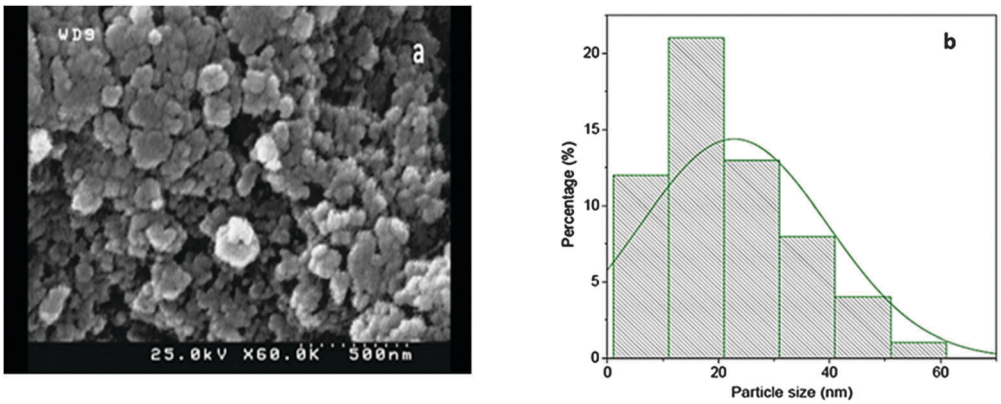

Fig. 3 SEM image (a), and particle size distribution (b) of the MSNs-HPZ-SO_3H.

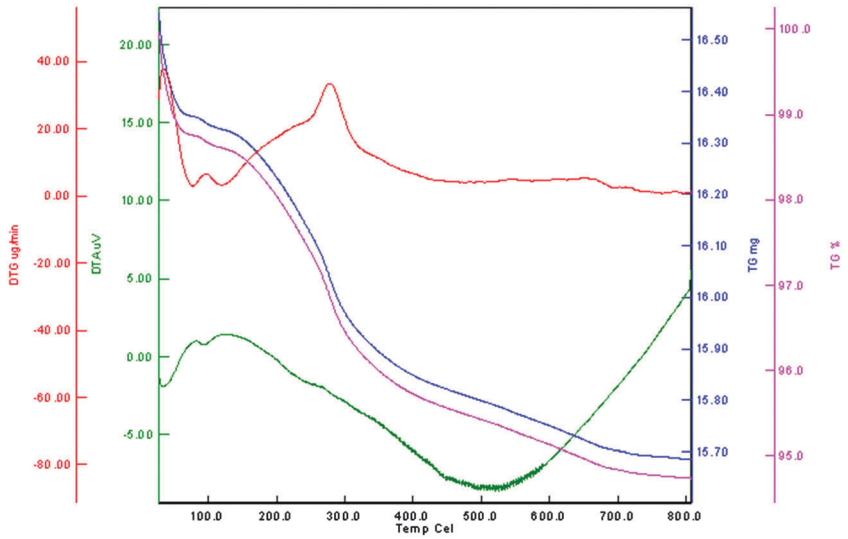

Fig. 4 TGA/DTA analyses for MSNs-HPZ-SO_3H nanocatalyst.

Thermogravimetric/differential thermal analyses (TGA/DTA) are presented in Fig. 4. In the TGA curve the weight loss from 25–120 °C can be assigned to the release of physically adsorbed water, solvent and organic groups on the external surface of nanoparticles. The weight loss between temperature ranges of 200–670 °C in the TGA curve are mainly associated with oxidative decomposition of organic and inorganic functional groups.

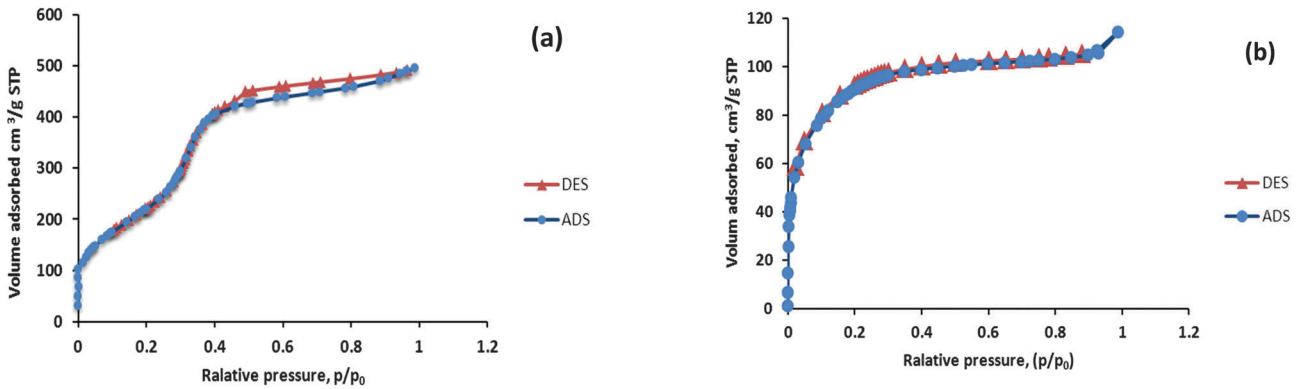

Fig. 5 N_2 adsorption/desorption isotherms: (a) MSNs, (b) MSNs-HPZ.

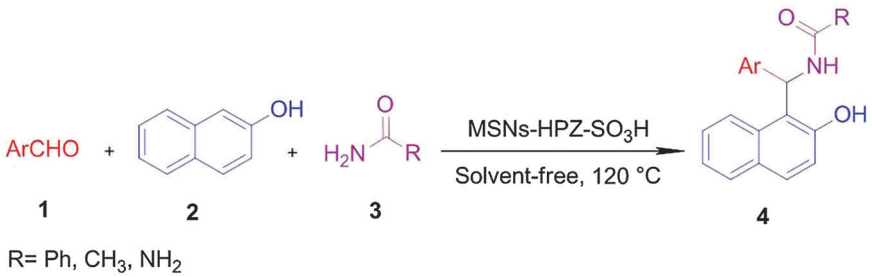

Scheme 2 Synthesis of 1-amidoalkyl-2-naphthols.

N_2 adsorption/desorption is a common method for characterization of mesoporous materials. It provide information about the specific surface area, average pore diameter and pore volume, *etc.* N_2 adsorption/desorption isotherms of MSNs and MSNs-HPZ are shown in Fig. 5. These isotherms exhibit type IV curve, which are characteristic of uniform mesoporous materials. The BET surface area, pore volume, and pore diameter of MSNs are 783 $m^2\ g^{-1}$, 0.767 $cm^3\ g^{-1}$, and 3.9 nm, respectively. The corresponding values for MSNs-HPZ are decreased to 313 $m^2\ g^{-1}$, 0.175 $cm^3\ g^{-1}$, and 2.2 nm, respectively. These observations indicate that the organic groups have successfully been anchored at the surface of the mesopores.

Catalytic activity of MSNs-HPZ-SO_3H in synthesis of 1-amidoalkyl-2-naphthols

After characterization of MSNs-HPZ-SO_3H, its role as a heterogeneous catalyst was evaluated in the exclusive synthesis of 1-amidoalkyl-2-naphthol derivatives (Scheme 2).

In order to optimize conditions for synthesis of 1-amidoalkyl-2-naphthols, reaction of benzaldehyde with β-naphthol and acetamide was selected as the model reaction. Effects of catalyst amount, solvent, and temperature was probed. At first, the model reaction studied with different amounts of catalyst (5, 10, 15, 20 mg) in various times under solvent-free conditions. The best result was obtained when reaction reached 94% conversion in 60 minutes with 10 mg catalyst. It is important to note that in the absence of the catalyst, only trace product detected (Table 1). To compare the effects of solutions to that of solvent-free conditions, we carried out the reaction in the absence and presence of solvents such as EtOH, CH_3CN, CH_2Cl_2, DMF, toluene, and *n*-hexane. Almost all the reactions were less efficient in the presence of solvent than in its absence, considering the reaction time and yield% (Table 2).

Table 1 Effect of the catalyst amount on the reaction of β-naphthol with acetamide and benzaldehyde at 120 °C

Entry	Catalyst (mg)	Time (min)	Yield[a] (%)
1	0	480	(Trace)
2	5	60	50
3	5	90	75
4	10	15	35
5	10	30	53
6	10	45	70
7	10	60	94
8	10	80	94
9	15	60	87
10	20	60	80

[a] Isolated yields.

Table 2 Solvent effects on reaction of β-naphthol, acetamide and benzaldehyde, in the presence of 10 mg of the catalyst

Entry	Solvent[a]	Temperature (°C)	Time (min)	Yield[b] (%)
1	CH_3CN	Reflux	240	53
2	EtOH	Reflux	240	75
3	CH_2Cl_2	Reflux	240	70
4	DMF	Reflux	240	60
5	Toluene	Reflux	240	30
6	*n*-Hexane	Reflux	240	50
7	Solvent free	120	60	94

[a] 2 ml solvent was used. [b] Isolated yields.

To determine the effect of temperature, condensation of β-naphthol with acetamide and benzaldehyde was examined in the presence of MSNs-HPZ-SO_3H at different temperatures. When the reaction temperature was varied from room temperature to 120 °C, the product yield gradually increased, with the highest yield being obtained at 120 °C (Fig. 6).

After optimizing the reaction conditions, three-component condensation of various aldehydes and amides with β-naphthol over MSNs-HPZ-SO_3H was carried out. The results showed a highly effective performance of the catalyst in the preparation of 1-aminoalkyl-2-naphthols (Table 3). In all cases, aromatic

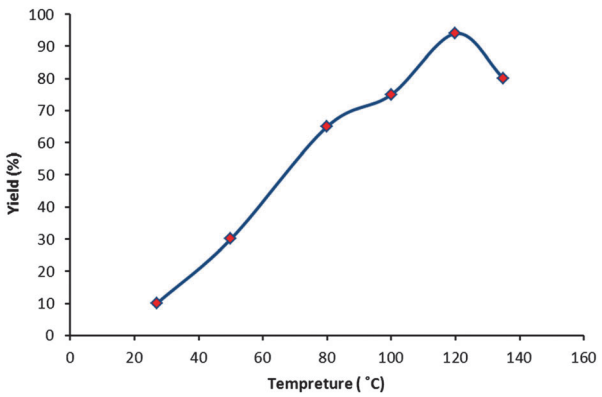

Fig. 6 Effect of temperature on the model reaction: (condensation of β-naphthol, benzaldehyde, and acetamide over MSNs-HPZ-SO_3H).

Table 3 Synthesis of 1-aminoalkyl-2-naphthols in the presence of MSNs-HPZ-SO_3H under solvent-free conditions

Entry	Ar	R	Time (min)	Yield[a] (%)	M.p. found (°C)	M.p. reported (°C)
1	Ph	CH_3	60	94	238–242	242–244 [ref. 34]
2	4-Cl–C_6H_4	CH_3	90	92	229–230	226–228 [ref. 34]
3	2-Cl–C_6H_4	CH_3	80	95	205–207	206–207 [ref. 19]
4	4-Me–C_6H_4	CH_3	100	85	210–212	212–213 [ref. 35]
5	3-NO_2–C_6H_4	CH_3	100	93	239–240	241–242 [ref. 34]
6	4-OMe–C_6H_4	CH_3	110	82	182–184	181–183 [ref. 34]
7	3-OMe–C_6H_4	CH_3	120	85	204–206	203–205 [ref. 34]
7	3-OH–C_6H_4	CH_3	105	90	225–228	227–229 [ref. 36]
8	4-OH–C_6H_4	CH_3	90	92	240–242	238–240 [ref. 36]
10	Ph	Ph	95	84	235–237	238–240 [ref. 19]
11	4-Cl–C_6H_4	Ph	100	91	180–182	179–181 [ref. 34]
12	2-Cl–C_6H_4	Ph	90	93	283–285	284–285 [ref. 19]
13	3-NO_2–C_6H_4	Ph	80	89	230–231	232–234 [ref. 37]
14	3-Br–C_6H_4	Ph	105	86	228–231	230–232 [ref. 37]
15	4-Me–C_6H_4	Ph	90	85	212–215	213–215 [ref. 34]
16	4-OH–C_6H_4	Ph	115	90	221–223	220–223 [ref. 37]
17	Ph	NH_2	90	82	176–178	175–177 [ref. 34]
18	3-OMe–C_6H_4	NH_2	100	86	166–169	167–169 [ref. 34]
19	3-NO_2–C_6H_4	NH_2	80	90	186–189	188–190 [ref. 38]
20	4-Cl–C_6H_4	NH_2	105	80	171–172	170–172 [ref. 38]

[a] Isolated yields.

aldehydes with substituent carrying either electron-donating or electron-withdrawing groups gave the products in excellent yields.

A plausible mechanism is proposed for the synthesis of 1-amidoalkyl-2-naphthols mediated over MSNs-HPZ-SO_3H (Scheme 3). The reaction proceeded *via* the formation of an intermediate *ortho*-quinonemethide (III). At first, nucleophilic addition of β-naphthol to the activated aldehydes by the nanocatalyst (complex I) obtain complex (II). The removal of water from complex (II) produces intermediate (III) as an *ortho*-quinone methide. The reaction activated intermediate (III) with amides *via* a Michael addition (complex IV) afford the expected amidoalkyl naphthols.

Reusability of MSNs-HPZ-SO_3H nanocatalyst

Reusability of MSNs-HPZ-SO_3H was investigated using model reaction. The catalyst was recovered after each run, washed thoroughly with ethanol, dried in an oven at 80 °C, for 4 h, and tested in the subsequent run. The procedure was repeated, and the results indicated that the catalyst could be recycled five times with a slight loss of its catalyst activity (Fig. 7).

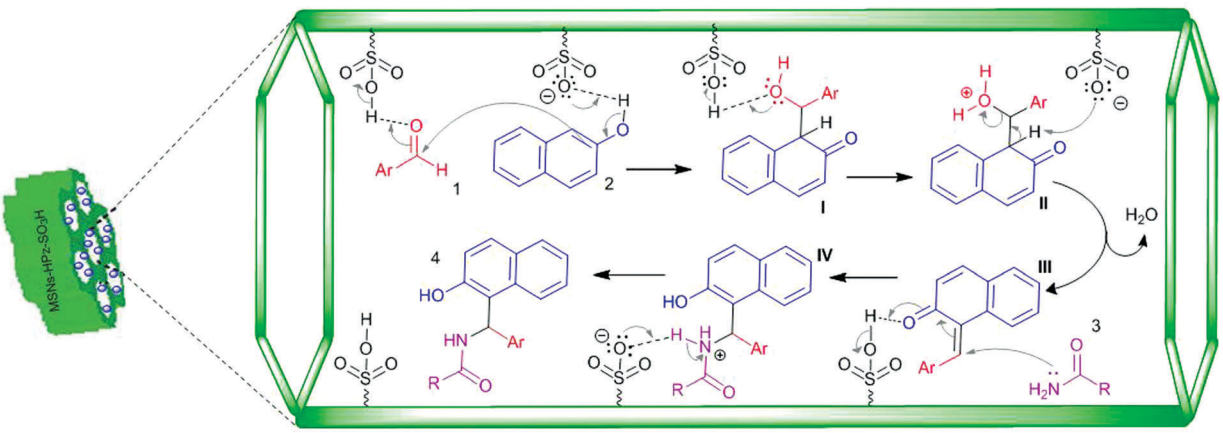

Scheme 3 Plausible mechanism for the synthesis of 1-aminoalkyl-2-naphthols using MSNs-HPZ-SO_3H.

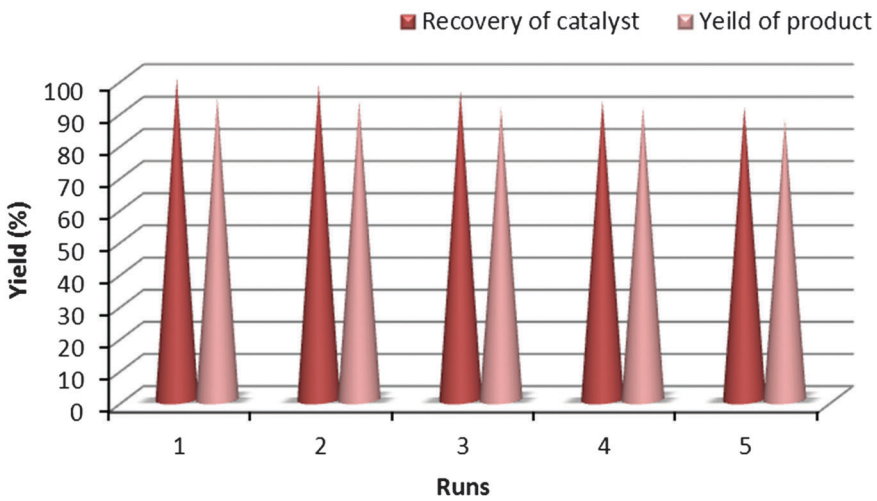

Fig. 7 Reusability of MSNs-HPZ-SO_3H nanocatalyst.

Conclusions

MSNs-HPZ-SO_3H was fabricated and fully characterized, then used as a new nanocatalyst in an efficient, one-pot preparation of 1-aminoalkyl-2-naphthols derivatives, from the three-component condensation reaction of various aromatic aldehydes, β-naphthol, and amide/urea, under thermal solvent-free conditions. The one-pot nature and the use of a heterogeneous solid acid material as the eco-friendly nanocatalyst make this protocol an interesting alternative to multi-step approaches. It offers several promising advantages such as high yield, easy handling, good reaction time, reusability of the nanocatalyst and compliance with the green chemistry. These advantages, in general, highlight this protocol as a useful and attractive methodology among of the methods reported in the literature, for the rapid synthesis of biologically active 1-amidoalkyl-2-naphthols.

Experimental

Materials and methods

Chemical reagents in high purity were purchased from Merck and Aldrich and used without further purification. Melting points were determined in open capillaries using an Electrothermal 9100 apparatus and are uncorrected. Fourier transform infrared (FT-IR) spectra were recorded using KBr pellets in the range 400–4000 cm^{-1} on a Nicolet IR-100 infrared spectrometer. The NMR spectra were recorded on a Brucker DRX 500-Avance spectrometer operating at 500 MHz for ^1H NMR in DMSO-d_6 with TMS as an internal standard. X-ray diffraction (XRD) was performed on Philips XPert 1710 diffractometer. The latter appeared with Co Kα (α = 1.79285 Å) voltage: 40 kV. Thermogravimetric/differential thermal analyses (TGA/DTA) were done on a thermal analyzer with a heating rate of 10 °C min^{-1} over a temperature range of 25–800 °C. The particle morphology was examined by scanning electron microscopy using SEM (HITACHI S-4160), on gold coated samples.

General procedure for the preparation of (MSNs)

MSNs was synthesized according to the sol–gel method.[33] Specifically, 0.5 g of CTAB and 0.14 g of NaOH were mixed in 240 mL deionized water. The solution was stirred vigorously at 80 °C for 2 h, then 2.5 mL of tetraethyl orthosilicate (TEOS) was added, and the reaction was continued for another 2 h. The as-prepared product (MSNs-CTAB) was washed 3 times with ethanol and re-dispersed in 200 mL of ethanol containing 2 g of NH_4NO_3, at 80 °C. The remaining mixture was refluxed for 6 h. In this process the CTAB template was removed. The resulting precipitate was collected by centrifugation and washed with ethanol repeatedly. Finally, it was dried under vacuum to give MSNs as a white powder.

General procedure for the preparation of (MSNs-Cl)

MSNs-Cl was prepared by refluxing 0.5 g of MSNs with 0.5 g of 3-chloropropyltrimethoxysilane (CPTMS) in toluene, under a nitrogen atmosphere, for 24 h. The resulting solid was filtered and washed with toluene, then dried under vacuum.

General procedure for the preparation of (MSNs-HPZ)

A solution of 1 g (10 mmol) of homopiperazine, in dry toluene and propyl amine, was added drop wise to a suspension of 0.5 g of the MSNs-Cl in toluene. The system was kept in reflux, under nitrogen atmosphere and stirring, for 24 h. At the end, the solid was filtered and washed in Soxhlet with 10 mL of *n*-butyl amine, then with 12 mL of diethyl ether and a dichloromethane solution. This procedure help to eliminate HCl, which otherwise would remain on the catalyst surface, and would deactivate it. After this treatment, MSNs-HPZ was dried under vacuum.

General procedure for the preparation of (MSNs-HPZ-SO_3H)

Finally for synthesis of MSNs-HPZ-SO_3H, to a solution of MSNs-HPZ (0.5 g) in *n*-hexane (2 mL), Et_3N (0. 1 mL) was added. The mixture was stirred for 5 min. Then, chlorosulfonic acid (0.1 mL) was added. The mixture was stirred for next 3 h for completing the reaction. Afterwards, the residue was filtered and washed with toluene, ethanol, water, and dried under vacuum.

Acidity of MSNs-HPZ-SO_3H

Titrations were utilized to determine the acid loading of the catalysts. At first, 100 mg of MSNs-HPZ-SO_3H was dispersed in 20 ml H_2O by sonicating for 40 min at room temperature after which the pH of solution was acidic, two drops of phenolphthalein indicator solution was added. The acidic solution was titrated to neutrality using 0.1 M NaOH solution to determine the loading of acid sites on the MSNs-HPZ-SO_3H catalyst. The results revealed that the samples of MSNs-HPZ-SO_3H possessed 2.1 mmol H^+ g^{-1}. This process was repeated for recovered catalyst after reaction, the results showed no substantial change in amount of acid loading of catalyst. Hence, no leaching of the acid occurred during the course of the reaction.

General procedure for the preparation of substituted 1-amidoalkyl-2-naphthols

A mixture of aldehyde (1 mmol), β-naphthol (1 mmol), amide/urea (1.2 mmol), and the catalyst (10 mg) were stirred at 120 °C, in an oil bath for the appropriate time. After completion of the reaction (monitored by TLC), the mixture was cooled to room temperature, the resulting solidified blend was diluted with hot ethanol and stirred for 5 min. The catalyst was filtered off, and the solution was concentrated under reduced pressure, to obtain the product which was recrystallized from ethanol. Products were characterized by spectral data and comparison of their physical data with the literature. Spectral data for *N*-[(3-methoxy phenyl)-(2-hydroxy-napthalen-1-yl)-methyl]-acetamide (Table 3, entry 7).

FT-IR (KBr, cm^{-1}): 3372, 3178, 3062, 1643, 1582, 1514, 1437, 1364, 1305, 1282, 1232, 1153, 1057, 989, 943, 863, 815, 748, 687, 614, 573; ^1H NMR (500 MHz, DMSO-d_6): δ (ppm) 1.97 (s, 3H, CH_3), 3.65 (s, 3H, OCH_3), 6.69–6.7 (m, 3H, ArH), 7.08–7.26 (m, 4H, ArH), 7.35 (t, 1H, ArH), 7.74–7.82 (m, 3H, ArH and CH), 8.44 (d, J = 10 Hz, 1H, NH), 9.99 (s, 1H, ArOH).

References

1 (*a*) A. Domling and I. Ugi, *Angew. Chem., Int. Ed.*, 2000, **39**, 3168–3210; (*b*) H. R. Hobbs and N. R. Thomas, *Chem. Rev.*, 2007, **107**, 2786–2820; (*c*) A. Domling, *Chem. Rev.*, 2006, **106**, 17–89; (*d*) D. Tejedor and F. Garcia-Tellado, *Chem. Soc. Rev.*, 2007, **36**, 484–491; (*e*) G. Shanthi and P. T. Perumal, *Tetrahedron Lett.*, 2009, **50**, 3959–3962.

2 S. Knapp, *Chem. Rev.*, 1995, **95**, 1859–1876.

3 Y. Kusakabe, J. Nagatsu, M. Shibuya, O. Kawaguchi, C. Hirose and S. Shirato, *J. Antibiot.*, 1972, **2**, 44–47.

4 S. Remillard, L. I. Rebhun, G. A. Howie and S. M. Kupchan, *Science*, 1975, **189**, 1002–1005.

5 G. Y. Lesher and A. R. Surrey, *J. Am. Chem. Soc.*, 1955, **77**, 636–641.

6 H. S. Mosher, M. B. Frankel and M. Gregory, *J. Am. Chem. Soc.*, 1953, **75**, 5326–5328.

7 J. L. Peglion, J. Vian, B. Gourment, N. Despaux, V. Audinot and M. Millan, *Bioorg. Med. Chem. Lett.*, 1997, **7**, 881–886.

8 H. Ren, S. Grady, D. Gamenara, H. Heinzen, P. Moyna, S. Croft, H. Kendrick, V. Yardley and G. Moyna, *Bioorg. Med. Chem. Lett.*, 2001, **11**, 1851–1854.

9 R. D. Clark, J. M. Caroon, A. F. Kluge, D. B. Repke, A. P. Roszkowski, A. M. Strosberg, S. Baker, S. M. Bitter and M. D. Okada, *J. Med. Chem.*, 1983, **26**, 657–661.

10 H. Matsuoka, N. Ohi, M. Mihara, H. Suzuki, K. Miyamoto, N. Maruyama, K. Tsuji, N. Kato, T. Akimoto, Y. Takeda, K. Yano and T. Kuroki, *J. Med. Chem.*, 1997, **40**, 105–111.

11 M. M. Khodaei, A. R. Khosropour and H. Moghanian, *Synlett*, 2006, 916–920.

12 S. Kantevari, S. V. Vuppalapati and L. Nagarapu, *Catal. Commun.*, 2007, **8**, 1857–1862.

13 B. Das, K. Laxminarayana, B. Ravikanth and B. R. Rao, *J. Mol. Catal. A: Chem.*, 2007, **261**, 180–183.

14 A. R. Supal and G. S. Gokavi, *J. Chem. Sci.*, 2010, **122**, 189–192.

15 M. Zandi and A. R. Sardarian, *C. R. Chim.*, 2012, **15**, 365–369.

16 G. H. Mahdavinia and M. A. Bigdeli, *Chin. Chem. Lett.*, 2009, **20**, 383–386.

17 M. Wang, Y. Liang, T. T. Zhang and J. J. Gao, *Chin. Chem. Lett.*, 2012, **23**, 65–68.

18 H. Hashemi and A. R. Sardarian, *J. Iran. Chem. Soc.*, 2013, **10**, 745–750.

19 G. C. Nandi, S. Samai, R. Kumar and M. Singh, *Tetrahedron Lett.*, 2009, **50**, 7220–7222.

20 M. Lei, L. Ma and L. Hu, *Tetrahedron Lett.*, 2009, **50**, 6393–6397.

21 H. R. Shaterian, H. Yarahmadi and M. Ghashang, *Tetrahedron*, 2008, **64**, 1263–1269.

22 D. Kundu, A. Majee and A. Hajra, *Catal. Commun.*, 2010, **11**, 1157–1159.

23 A. R. Hajipour, Y. Ghayeb, N. Sheikhan and A. E. Ruoho, *Tetrahedron Lett.*, 2009, **50**, 5649–5651.

24 B. M. Pereza, J. Roeserb, A. Thomasb and P. Hesemanna, *Appl. Organomet. Chem.*, 2013, **27**, 290–299.

25 E. Merino, E. V. Sesto, E. M. Maya, M. Iglesias, F. Sanchez and A. Corma, *Chem. Mater.*, 2013, **25**, 981–988.

26 A. Comotti, S. Bracco, P. Valsesia, L. Ferretti and P. Sozzani, *J. Am. Chem. Soc.*, 2007, **129**, 8566–8576.

27 M. Sharifi, C. Kohler, P. Tolle, T. Frauenheim and M. Wark, *Small*, 2011, **7**, 1086–1097.

28 P. J. Lebed, J. D. Savoie, J. Florek, F. Bilodeau, D. Lariviere and F. Kleitz, *Chem. Mater.*, 2012, **24**, 4166–4176.

29 N. Mizoshita, K. I. Yamanaka, S. Hiroto, H. Shinokubo, T. Tani and S. Inagaki, *Langmuir*, 2012, **28**, 3987–3994.

30 N. A. Brunelli, K. Venkatasubbaiah and C. W. Jones, *Chem. Mater.*, 2012, **24**, 2433–2442.

31 K. Liu, R. Jin, T. Cheng, X. Xu, F. Gao, G. Liu and H. Li, *Chem. – Eur. J.*, 2012, **18**, 15546–15553.

32 M. Sasidharan and A. Bhaumik, *ACS Appl. Mater. Interfaces*, 2013, **5**, 2618–2625.

33 I. I. Slowing, B. G. Trewyn and V. S. Y. Lin, *J. Am. Chem. Soc.*, 2007, **129**, 8845–8849.

34 Q. Zhang and J. Luo andY. Wei, *Green Chem.*, 2010, **12**, 2246–2254.

35 H. Moghanian, A. Mobinikhaledi, A. G. Blackmanc and E. Sarough-Farahanib, *RSC Adv.*, 2014, **4**, 28176–28185.

36 A. Ghorbani-Choghamarani and S. Rashidimoghadam, *Chin. J. Catal.*, 2014, **35**, 1024–1029.

37 R. Tayebee, M. Amini, M. Akbari and A. Aliakbari, *Dalton Trans.*, 2015, **44**, 9596–9609.

38 M. Esmaeilpour, J. Javidi and M. Zandi, *Mater. Res. Bull.*, 2014, **55**, 78–87.